Bioorganic & Medicinal Chemistry 27 (2019) 525–532

Contents lists available at ScienceDirect

Bioorganic & Medicinal Chemistry

journal homepage: www.elsevier.com/locate/bmc

Acid-controlled release complexes of podophyllotoxin and etoposide with acyclic cucurbit[*n*]urils for low cytotoxicity

Fanjie Li[a,c], Dan Liu[a,c], Xiali Liao[a], Yulin Zhao[b], Rongtao Li[a], Bo Yang[a,*]

[a] Faculty of Life Science and Technology, Kunming University of Science and Technology, Kunming 650500, PR China
[b] Faculty of Chemical Engineering, Kunming University of Science and Technology, Kunming 650500, PR China

ARTICLE INFO

Keywords:
Acid-controlled release
Acyclic cucurbit[*n*]uril
Podophyllotoxin and etoposide
Inclusion complex
Low cytotoxicity

ABSTRACT

The targeted or responsive systems are appealing therapeutic platforms for the development of next-generation precision medications. So, we design and prepare acid-controlled release complexes of podophyllotoxin (POD) and etoposide (VP-16) with pH-labile acyclic cucurbit[*n*]urils, and their characteristics and inclusion complexation behaviors were investigated via fluorescence spectroscopy, nuclear magnetic resonance and X-ray power diffraction. Cells incubated with complexes have been analyzed by high-content analysis (HCA), and cytotoxicity tests have been completed by MTT assay. The results showed that complexes with different binding constants can release the drug substance in the physiological pH environment of cancer cells, maintain good anticancer activity, and have low cytotoxicity. This provides a strategy about targeted and responsive systems of POD and VP-16 for clinical application.

1. Introduction

Discussions on increasing anticancer activity and reducing side effects of normal cells of anticancer agents have existed in recent years. Molecular containers as potential drug carriers attracted a lot of attention. The prevailing molecular container compounds include crown ethers, cryptands, carcerands, calixarenes, cyclophanes, cyclodextrins, cucurbituril, and complexes self-assembled by metal-ligand and H-bonding interactions and reversible covalent bonds.[1] In general, supramolecular containers have a hollow three-dimensional structure with a hydrophobic internal cavity and hydrophilic external surface.[2] They can form host-guest inclusion complexes with molecules having suitable size by self-assembly. In this investigation, we aim to study host–guest interactions between acyclic cucurbit[*n*]uril with pH stimulus-responsive function and anti-cancer drugs. Therefore, we disclose the synthesis of stimulus-response acyclic cucurbit[*n*]uril and used to increase drug solubility and targeted drug delivery (Fig. 1).[3] From Fig. 1, under mildly acidic conditions (pH 5.5–6.5), host-1 can degrade into the host-2 and release encapsulated cargoes at an accelerated rate due to the decrease in binding capacity.[3] In other words, when host-1 is delivered onto the surface of tumor cells, anticancer drugs will be released to play an active role due to mildly acidic conditions of tumor tissues. As a result, smart stimuli-responsive supramolecular inclusion complexes have a promising application potential in the therapy of tumors and relevant diseases.[4,5]

Podophyllotoxin (POD, Fig. 1), a natural compound derived from the roots of *Podophyllum pleianthum*,[6] contains four consecutive chiral centers and four nearly planar fused rings. This compound has traditionally and commonly been isolated from podophyllin, resin of Podophyllum rhizome.[7,8] It is also an important natural product in lignan.[9,10] POD is widely studied and applied due to its excellent biological activity such as effective inhibition of herpes virus,[11–13] therapy of toxic sexually transmitted diseases,[14–16] treatment of condyloma acuminate,[17–19] etc. The most important thing is that POD has also been proved to be effective in cancer therapy.[8,20] Many studies have shown that it had good antitumor activity against different tumor cell lines (such as P-388 murine leukemia, A-549 human lung carcinoma, HT-29 human colon carcinoma and MEL-28 human melanoma).[21] What the mechanism of its antineoplastic and antiviral properties is that it can lead to the inhibition of tubulin polymerization and the arrest of the cell cycle in the metaphase.[7,22] Unfortunately, it is also lethal to normal cells and it has a very low water solubility, which prevent it from being used in clinical research.[23] To overcome these shortcomings, podophyllotoxin derivatives have been extensively studied.[24–28] Lots of POD derivatives, such as etoposide, teniposide, and etopophos, have been developed for achieving higher antitumor activity, better water-solubility, and few side effects. Although great efforts were made to improve its water solubility and cytotoxicity, it's still worthy of further

* Corresponding author.
E-mail address: yangbo6910@sina.com (B. Yang).
[c] These authors contributed equally to this work.

https://doi.org/10.1016/j.bmc.2018.12.035
Received 9 November 2018; Received in revised form 14 December 2018; Accepted 27 December 2018
Available online 28 December 2018

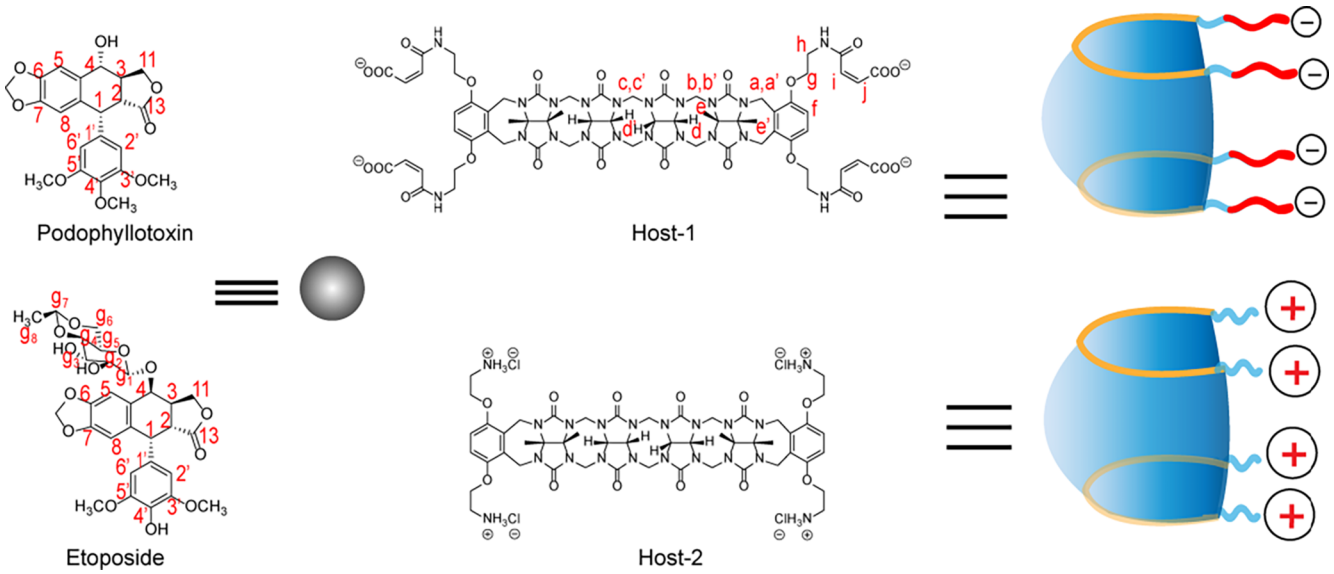

Fig. 1. The structures of Podophyllotoxin, Etoposide, Host-2 and Host-1.

research. Therefore, it is important to develop delivery systems for the wide clinical application of podophyllotoxin and its derivatives. In order to solve the above problems, we investigated the interaction of POD with the host-1. In addition, etoposide (VP-16, Fig. 1), a derivative of podophyllotoxin synthesized in the 1960s, is a topoisomerase II inhibitor, which can prohibit the function of topoisomerase II-DNA and stop the cell cycle at the late S and G2 phases.[29] Since VP-16 was discovered, its application in the treatment of human malignancies has continued to increase, and it has become an essential antitumor drug. Moreover, etoposide, as a part of an important second-line drug, can treat a variety of malignancies including small cell lung cancer,[30] non-hodgkin's lymphoma,[31] hodgkin's disease,[32] non-lymphocytic leukaemia,[29] ovarian,[32] and kaposi's sarcoma.[33] In addition, etoposide is part of an important second-line drug or remedy for several cancer treatments.[29] However, low water-solubility and bioavailability limit its application in cancer treatment. Therefore, the construction of efficient and nontoxic carriers for the delivery of VP-16 has become an important step in its further clinical application. Our group has reported the use of cyclodextrin to form inclusion complexes with POD by host-guest chemistry to increase its water solubility.[34] However, this merely solves its water solubility and the side effects which restrict its clinical application not resolved.

In order to improve the water-solubility, absolute bioavailability and tumor targeting performance of POD and VP-16, we investigated the interaction of POD and VP-16 with host-1 in aqueous solution. Binding behaviors of native host-1 with POD and VP-16 and the solubilization effect of host-1 toward POD and VP-16 were also explored, which provided a highly effective approach to construct novel POD and VP-16 formulations with high bioavailability. Moreover, mildly acidic environments in tumor tissues could cause the degradation of host-1 and the release of cargoes. As a result, inclusion complexes of host-1 with POD and VP-16 can precisely deliver drugs to tumor cells to achieve targeted drug delivery, which has potential application value and significance in tumor treatment.

2. Experimental

2.1. Reagents and materials

All the reagents were purchased from commercial sources and used without further purification. POD (molecular weight = 414.41, PC > 98%) and VP-16 (molecular weight = 588.56, PC > 99%) used in this work was purchased from the National Institute for Control of Pharmaceutical. Other reagents were of analytical grade. All experiments were carried out by using ultra-pure water.

2.2. Synthesis of host-1

Host-2 was synthesized according to the previous literature[35] (see supporting information). The procedure for the preparation of host-1 was given in the following text as a typical example. Host-2 (1.48 g, 1.15 mmol) was dissolved in ultra-pure water (18 ml). Triethylamine was added and it was stirred at room temperature for 10 min. Subsequently, maleic anhydride (3.58 g, 35.45 mmol) was added and dissolved in acetonitrile (0.6 ml). The mixture was stirred at room temperature for 8 h. The reaction solution was adjusted to pH 6.0 with HCl (1 M) solution. The precipitate was collected by centrifugation and washed with acetone (75 ml × 2). The obtained white solid was dissolved in water, and the pH was adjusted to 7.4 with a NaOH (1 M) solution. The solvent was removed on a rotary evaporator to give a host-1 as a white solid (1.68 g, 1.04 mmol, 87%). Proton nuclear magnetic resonance (Supporting information, Fig. S5) (^{1}H NMR, 600 MHz, D_2O): 6.56 (s, 4H), 6.21 (d, 4H, J = 12.4 Hz), 5.90 (d, 4H, J = 12.4 Hz), 5.51 (d, 2H, J = 15.4 Hz), 5.45 (d, 4H, J = 16.2 Hz), 5.31 (d, 2H, J = 9.2 Hz), 5.24 (d, 2H, J = 9.2 Hz), 5.18 Hz (d, 4H, J = 15.8 Hz), 4.16 (d, 4H, J = 15.8 Hz), 4.11 (d, 4H, J = 16.2 Hz), 3.97 (d, 2H, J = 15.4 Hz), 3.85 (m, 4H), 3.64 (m, 4H), 3.33 (m, 8H), 1.68 (s, 6H), 1.66 (s, 6H).

2.3. Preparation of POD/host-1 and VP-16/host-1 supramolecular system

The POD/host-1, VP-16/host-1 inclusion complex were prepared in aqueous solution. Host-1 (200 mg) was dissolved in 10 ml ultra-pure water and the required amount of POD (or VP-16) was added to obtain a 1:3 mol ratio. The mixture was stirred for 7 days at room temperature in the dark, and the undissolved POD or VP-16 were removed by micro porous filter membrane (0.22 μm). The filtrate was evaporated under reduced pressure and dried under vacuum to give the POD/host-1, VP-16/host-1 inclusion complexes.

2.4. Preparation of physical mixtures

A physical mixture of Host-1 and POD, VP-16 was prepared. The molar ratio of host-1 to guest molecule was 1:1. After grinding in a

mortar for 10 min, the physical mixture of host-1 and guest molecule was obtained.

2.5. ^1H NMR analysis

NMR experiments were carried out in $CDCl_3$ or D_2O. Tetramethylsilane (TMS) was used as a reference in D_2O. The samples were dissolved in 99.98% D_2O or 99.98% $CDCl_3$ and filtered before use. ^1H NMR spectra were acquired on a Bruker Avance III HD spectrometer (600 MHz) at 25 °C. The one-dimensional spectra of both solutions were run with FID resolution of 0.18 Hz/point. The residual HDO line had a line width at a half-height of 2.59 Hz.

2.6. Preparation of samples for Job's plots and complex constant

The stoichiometric relationship between host-1 and guest was determined by Job's curve method.[36] We used fluorescence spectroscopy to monitor the continuously changing data. The total molar concentration of host-1 and guest remains unchanged. And the molar fraction of the guest varies from 0.1 to 0.9. The fluorescence intensity of the solution at different mole fractions was monitored separately.

2.7. Fluorescence spectroscopy

Fluorescence absorption spectroscopy measurements were performed by using a Shimadzu RF-5301 pc in a constant temperature compartment using a conventional 1 cm path (1 cm × 1 cm × 4 cm) quartz cell maintained at 25 °C by Shimadzu TB-85 Thermo. Spectral titration was performed by the following steps: POD (1.0×10^{-6} M) and host-1 (1.0×10^{-4} M) solution were provided in a buffer solution (KH_2PO_4-NaOH, pH7.4). The concentration of POD was held constant at 1.0×10^{-6} M. Then, an appropriate amount of host-1 was added, and the final concentrations varied from 0 to 0.0297 mM (host-1: 0.0000, 0.0017, 0.0033, 0.0050, 0.0083, 0.0115, 0.0147, 0.0208, 0.0297 mM at pH 7.4. The absorption spectra measurements were taken after 1 h. Spectral titration was performed by the following steps: VP-16 (1.0×10^{-7} M) and host-1 (1.0×10^{-5} M) solution were provided in a buffer solution (KH_2PO_4-NaOH, pH7.4). The concentration of VP-16 was held constant at 1.0×10^{-7} M. Then, an appropriate amount of host-1 was added, and the final concentrations varied from 0 to 0.0297 mM (host-1: 0.0000, 0.0001, 0.0007, 0.0014, 0.0041, 0.0078, 0.0144, 0.0248, 0.0446, 0.0632 mM at pH 7.4). The absorption spectra measurements were taken after 1 h. Measurements were made in the 220–700 nm spectral range. All experiments were carried out in triplicate.

2.8. Powder X-ray diffraction (XRD)

The XRD patterns were obtained by using a D/Max-3B diffractometer with Cu Kα radiation (40 kV, 100 mA), at a scanning rate of 5°/min. Powder samples were mounted on a vitreous sample holder and scanned with a step size of 2θ = 0.02° between 2θ = 5° and 60°.

2.9. Host-1 degradation

Use ^1H NMR to monitor the degradation of the host under acidic conditions. We incubated host-1 at 37 °C and pD 5.0 for 3 h, 6 h and 3 d, respectively. Then we performed ^1H NMR studies on the incubated product.

2.10. Cell culture study

Here we have selected four human cells (HCT116, HepG2, SY5Y, 293T). Doxorubicin and cisplatin were used as the positive control. Cells were suspended in RPMI 1640 (Hyclone Corp. Utah, USA) supplemented with 10% fetal bovine serum (Hyclone) at 37 °C in a humidified atmosphere of 5% CO_2 in air. Afterward, cells were seeded into 96-well microculture plates. Culture for 24 h, drugs, host-1 and host-1/drugs inclusion complexes was then added, respectively. After 48 h exposure to the compounds, cells viability was determined by the [3-(4,5-dimethylthiazol-2-yl)-2,5-diphenyltetrazolium bromide] (MTT) cytotoxicity assay by measuring the absorbance at 490 nm with a microplate spectrophotometer. Each test was performed in triplicate.

Studying on the release of cargo at different pH values, we used free rhodamine B or host-1/rhodamine B inclusion complexes incubated with HepG2 cells at 37 °C 1 h in difference pH value. The medium was adjusted to pH 6.4 and 5.5 with dilute hydrochloric acid. Subsequently, cells were washed five times with PBS to remove surface-bound rhodamine B molecules. Cells were imaged by high content analysis with high throughput cell analyzer (Thermo Scientific Array Scan XTI).

3. Results and discussion

3.1. ^1H NMR analysis

^1H NMR spectroscopy studies were used to give a deep insight into the host-guest interactions. The addition of 3 eq. of POD (or VP-16) was added to a solution of host-1 in D_2O (6.2×10^{-3} M). POD and VP-16 is transparent to ^1H NMR under most conditions when D_2O is used as a solvent, owing to its poor water solubility. Assessment of the POD complex by ^1H NMR clearly demonstrated the presence of the framework protons of the POD molecule, which was consistent with the significant solubilization (Fig. 2). Comparing Fig. 2b with Fig. 2c, we could clearly see that some of the protons of podophyllotoxin have been shifted, due to the shielding effect of the electronrich host-1 cavity. The proton resonances of host-1 also displayed slight changes in their chemical shifts as well as significant signal broadening because of complexation dynamics between host-1 and POD. The changes in the ^{1}HNMR spectra indicate that POD was completely encapsulated within the host-1 cavity. Like Podophyllotoxin, VP-16 complex by ^1H NMR also clearly demonstrated the presence of the framework protons of the VP-16 molecule, which was consistent with the significant solubilization (Fig. 3). Comparing Fig. 3, we could find that the protons of the VP-16 and host-1 have been shifted. From the ^1H NMR changes, we can assure that VP-16 has entered the cavity of the host-1.

3.2. Stoichiometry

The stoichiometry between the host and guest can be effectively measured by the Job's plots. In this work, Job's plot was employed to obtain the stoichiometry of guest and host-1 via the fluorescence spectrometer. The concentration of guest solution (1×10^{-6} M) was kept constant, and it changed the concentration of the host-1 so that the mole fraction of guest (guest/[guest + host − 1]) varies between 0.1 and 0.9. In the concentration range, the Job's plot showed a maximum at a molar fraction of 0.5 (Fig. 4), proving the 1:1 inclusion complexation between POD and host-1. Similarly, VP-16 and host-1 Job's plot showed a maximum at a molar fraction of 0.5 (Fig. 4), proving the 1:1 inclusion complexation between VP-16 and host-1.

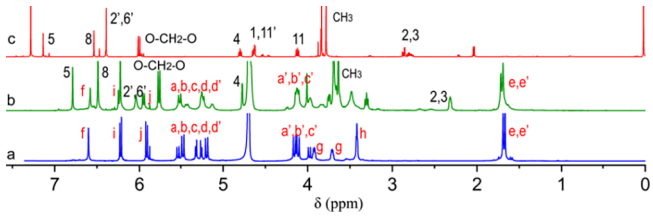

Fig. 2. ^1H NMR spectra of (a) host-1 in D_2O, (b) host-1/POD inclusion complex in D_2O, (c) POD in $CDCl_3$ at 25 °C.

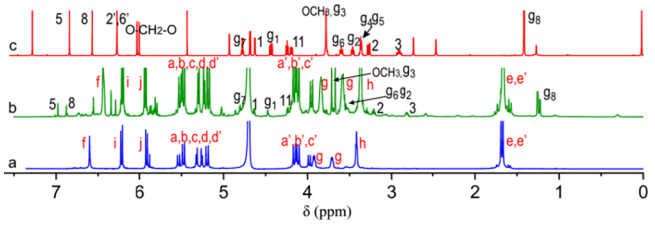

Fig. 3. ^{1}H NMR spectra of (a) host-1 in D_2O, (b) host-1/VP-16 inclusion complex in D_2O, (c) VP-16 in $CDCl_3$ at 25 °C.

3.3. Spectral titration

$$H+ G \overset{Ks}{\rightleftharpoons} H{\cdot}G \quad (1)$$

$$K_S = [G/H]/([G][H]) = (\Delta_A/\Delta_\varepsilon)/\{([G]^0 - \Delta_A/\Delta_\varepsilon)([H]^0 - \Delta_A/\varepsilon)\} \quad (2)$$

$$\Delta_A = \Delta_\varepsilon{\cdot}\{1/2[H]^0 + [G]^0 + 1/K_S - \sqrt{1/4([H]^0 + [G]^0 + 1/K_S) - [H]^0{\cdot}[G]^0}\} \quad (3)$$

$[H]^0$: initial host concentration; $[G]^0$: initial guest concentration; Δ_A: change of absorbance; ε: change of coefficiency; K_s: binding constant.

The inclusion complexation of host-1 with guest was quantitatively studied in buffer solution (KH_2PO_4-NaOH, pH7.4) by fluorescence spectrophotometry. From the change in the intensity of the fluorescence induced by the addition of the host molecule, we can determine the binding constants (Ks) of the complexes. From the Job curve experiment, we can know that the host-1 and the guest molecule POD (or VP-16) inclusion ratio is 1:1, so we can use Eq. (1) to determine their binding constants. The complex binding constants (Ks) were calculated for each host–guest combination from the nonlinear squares fit to Eq. (2). Where host-1 and guest refer to the total concentrations of the guest and host-1, respectively, the Eq. (2) on the basis of the completion of the Eq. (3). Finally, the Ks was obtained from the analysis of the sequential changes of the fluorescence intensity (Δintensity) at various host-1 concentrations, with a nonlinear least squares method according to the curve-fitting Eq. (3). As showed in Fig. S8, the fluorescence intensity of guest increases with the solubility of the host-1 and remained constant when the host-1 and the guest were saturated. Using a nonlinear least squares curve-fitting method, we obtained the binding constants for the host-1-guest inclusion complex. Fig. S8b illustrates a typical curve-fitting plot for the titration of POD with host-1, which shows the excellent fit between the experimental and calculated data and the 1:1 stoichiometry of the POD/host-1 inclusion complex. The binding constant of the complex was $(5.09 \times 0.12) \times 10^4\,M^{-1}$. Fig. S9 illustrates a typical curve-fitting plot for the titration of VP-16 with host-1, which shows the excellent fit between the experimental and calculated data and the 1:1 stoichiometry of the VP-16/host-1 inclusion complex. The binding constant of the complex was $(2.22 \times 0.08) \times 10^4\,M^{-1}$ (Table 1).

Table 1
Complex stability constants (Ks) and Gibbs free energy change $-\Delta G$ (KJ mol^{-1}) for 1:1 inclusion complexes of guest artesunate with host in PBS (pH 7.4) at 25 °C.

	Ks (M^{-1})	logKs	$-\Delta G$ (KJ mol^{-1})
Host-1/POD	$(5.09 \pm 0.12) \times 10^4$	4.7	26.85
Host-1/VP-16	$(2.22 \pm 0.08) \times 10^4$	4.3	24.79
Host-2/POD	0	N/A	N/A
Host-2/vp-16	0	N/A	N/A

On the other hand, inclusion complex between POD and VP-16 was not formed from NMR analysis. So, we could think that the binding constants of host-2 and POD (or VP-16) were 0 respectively. Thus, we suspect that during the mildly acid conditions, host-1 will be slowly released during the process of cleavage of host-1 into host-2. This is similar to the mildly acidity of the microenvironment of the tumor. Then we could design a targeted drug delivery system for tumor cells. We suspect that the drugs release was shown in Fig. 5. The following experiment will further demonstrate that the drugs in the inclusion compound will slowly release under mildly acidic conditions.

3.4. XRD analysis

X-ray power diffraction (XRD) was used to examine the crystalline state of host-1, host-1/guest physical mixture, host-1/guest inclusion complex and guest. As shown in Fig. 6, host-1 (Fig. 6a), POD (Fig. 6b) is in crystalline form. The XRD pattern of the physical mixture confirmed the presence of both species as isolated solids, as the diffractogram showed both POD peaks and host-1 peaks (Fig. 6c). The inclusion complexes noted an amorphous halo pattern from the diffractogram, in which the sharp diffraction peaks of POD completely disappeared (Fig. 6d). These results further proved that POD had been incorporated into the cavity of host-1 and presented as the amorphous or disordered structure. As shown in Fig. S7, free VP-16 is a crystalline solid (Supporting information, Fig. S10b). The XRD pattern of the physical mixture confirmed the presence of both species as isolated solids, as the diffractogram showed both VP-16 peaks and host-1 peaks (Supporting information, Fig. S10c). The lyophilized inclusion complex has an amorphous structure (Supporting information, Fig. S10d), probably due to both the structure of host-1 and the lyophilization process; this is evidence of the absence of VP-16 crystalline particles.

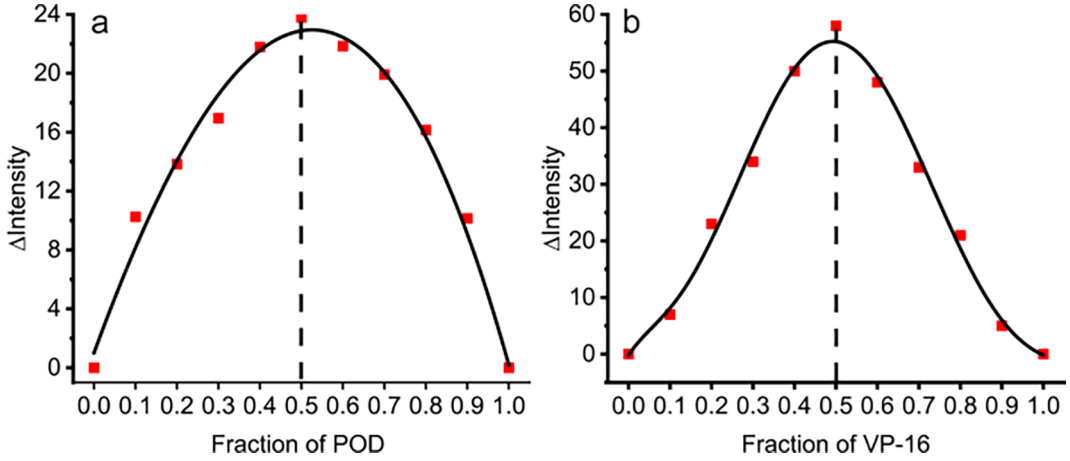

Fig. 4. Job's plots by fluorescence spectrometer for the binding stoichiometry of host-1 with POD (a), VP-16 (b).

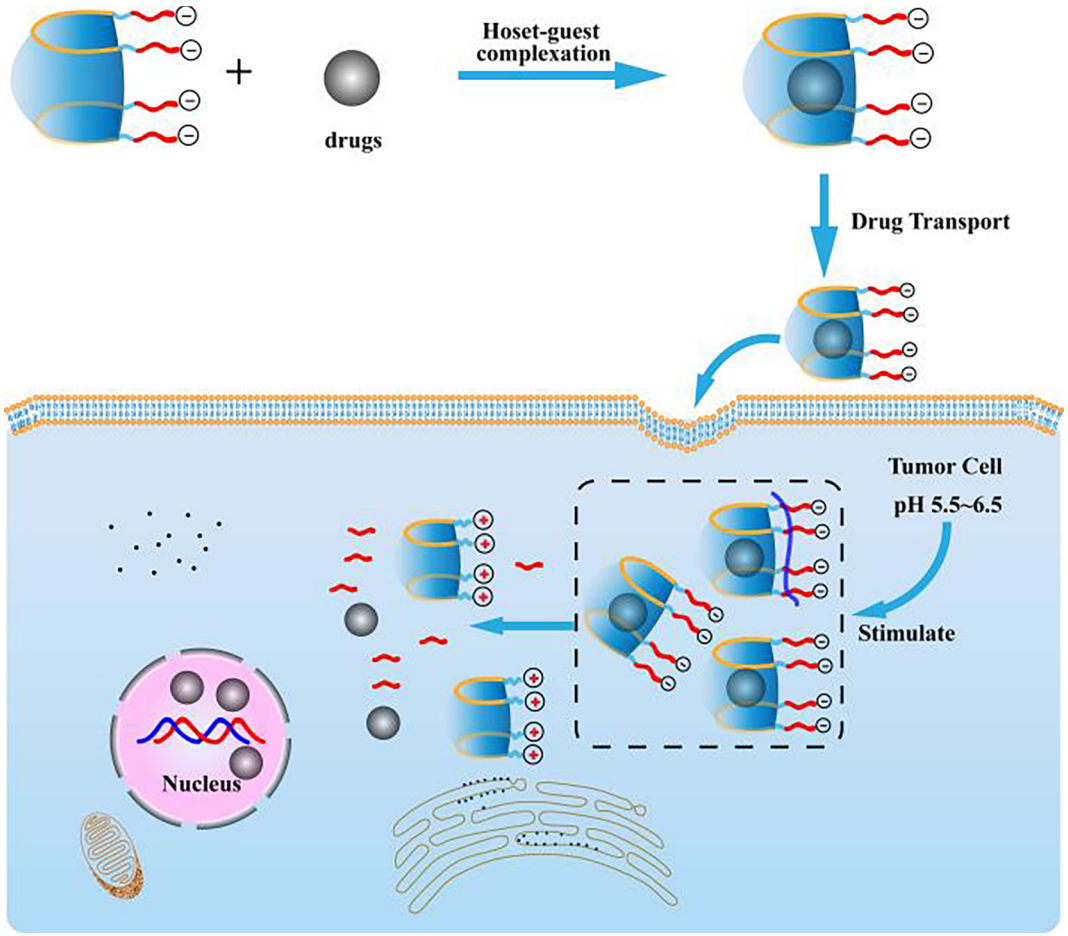

Fig. 5. Host-1 and drug combination and *in vivo* release schematic diagram.

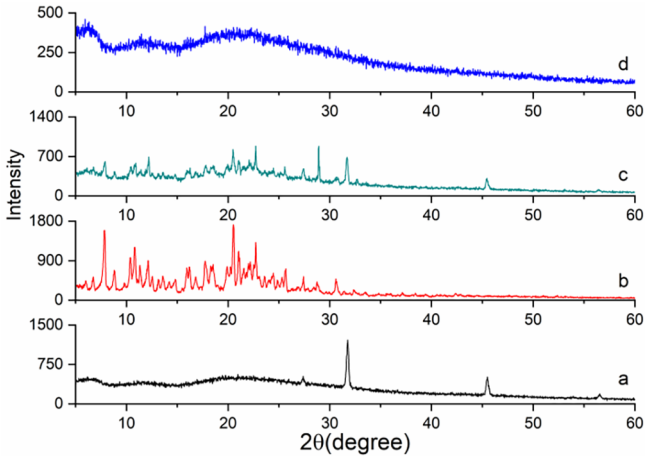

Fig. 6. Powder X-ray diffractograms for: (a) host-1, (b) POD, (c) host-1/POD 1:1 (mol proportion) physical mixture, (d) host-1/POD inclusion complex.

3.5. Host-1 degrade and drug release

As showed in Fig. 7, a small portion of the product was decomposed at 3 h incubation. From this ^{1}H NMR, it was observed that both the product and the raw material exist (Fig. 7b). After degradation for 6 h, it was manifestly seen that most of the host-1 was degraded. Meanwhile, it could be seen from the ^{1}H NMR that the content of the host-1 was significantly less than that of the incubation for 3 h (Fig. 7c). After degradation for 3 d, we observed a near complete conversion of host-1 to host-2 (Fig. 7d). This observation confirms that the degradation under acidic condition and "charge conversion" from anionic container to cationic container lead to the guest dissociation.[37] When the host-1 was lysed, the drugs entrapped inside were released and the targeted delivery of the drug was achieved.

We used ^{1}H NMR to demonstrate that host-1 degrade under acidic conditions and releases drug molecules. From Fig. 8, as the incubation time of the VP-16/host-1 inclusion complex under acidic conditions was gradually increased, the drug content gradually decreased. When the host-1 was completely cleaved, the hydrogen proton signal of the drug molecule was not visible from the NMR spectra. Host-1 can be cleaved to host-2 under acidic conditions and that host-2 cannot continue to wrap the drug to form a drug release.

3.6. In vitro cytotoxicity studies

The IC50 values, which represented the concentration of a drug required for 50% reduction of cellular growth, had been calculated and showed in Table 2. The evaluation was performed by MTT assay using doxorubicin and cisplatin as the positive control. It could be seen from the table that the inclusion complexes exhibited good cytotoxicity and were less toxic than the drug alone. Consequently, the inclusion complex could reduce the toxicity of the drugs to the cells, and the inclusion complexes were not toxic to 293T. The inclusion complex has low toxicity to normal cells and maintains good activity against tumor cells.

In order to study host-1 and to achieve in vitro release of anti-tumor drugs, we designed an in vitro uptake assay for HepG2 cells. Rhodamine B is used as a model drug, because it is the most commonly used as fluorescent substance in fluorescence analysis. To mimic the normal

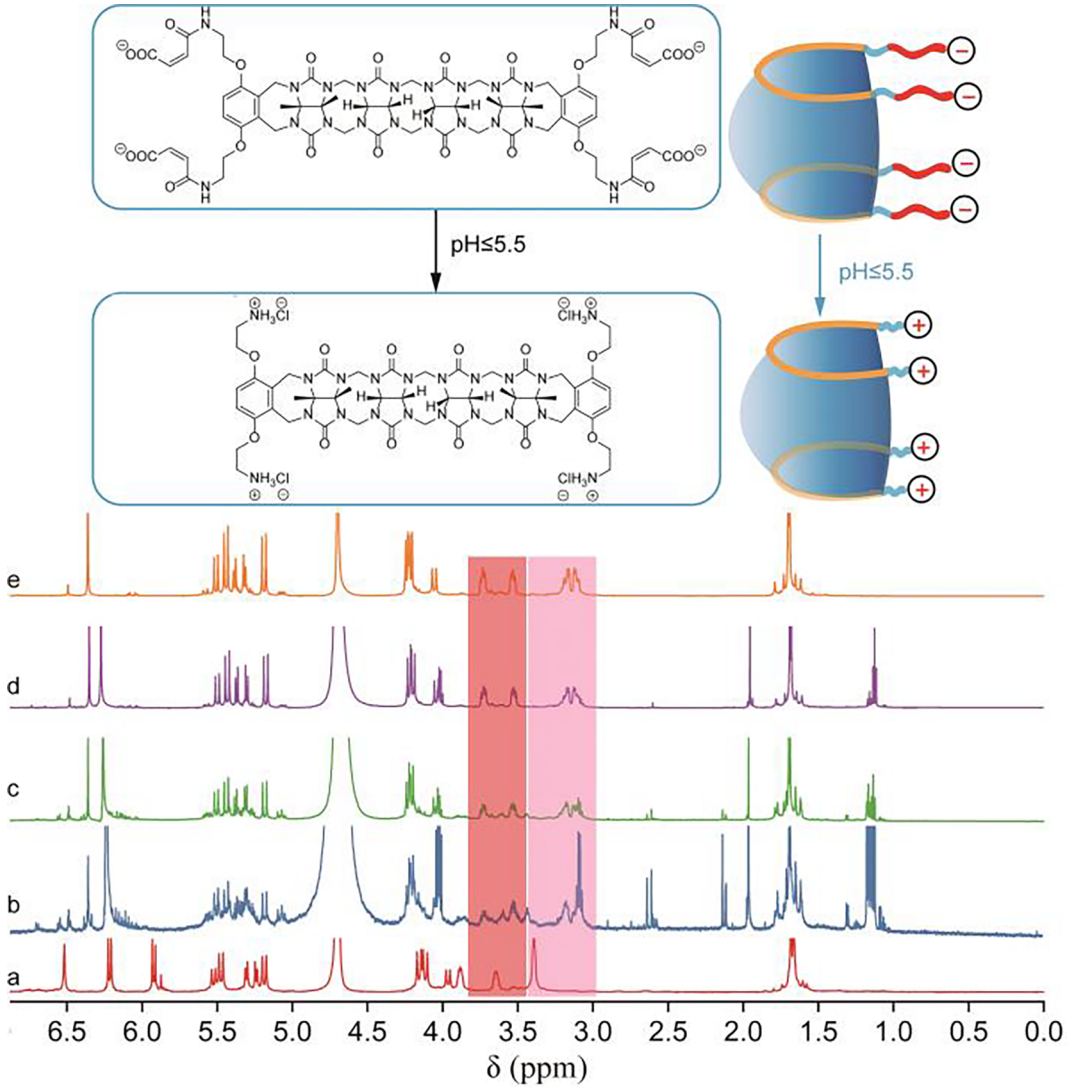

Fig. 7. ^{1}H NMR spectra of host-1 in D_2O for 0 h (a), after incubation in pD 5.0 buffer for 3 h (b), after incubation in pD 5.0 buffer for 6 h (c), and after incubation in pD 5.0 buffer for 3 d (d). and host-2 in pD 7.2 buffer (e). The shadow region indicates the complete degradation of host-1 and host-2.

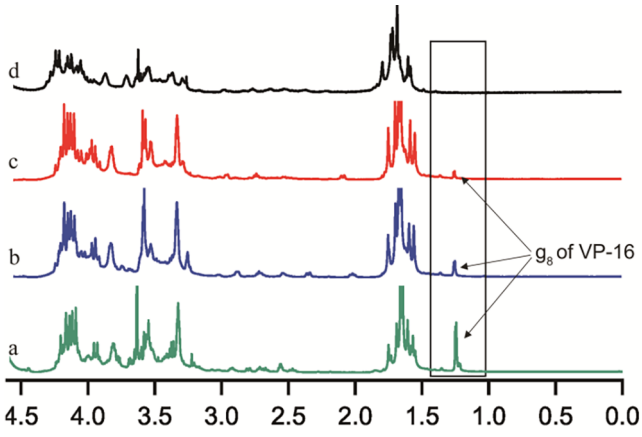

Fig. 8. ^{1}H NMR spectra of POD/host-1 inclusion complex in pD 5.0 buffer for 1 h (a), after incubation in pD 5.0 buffer for 3 h (b), after incubation in pD 5.0 buffer for 6 h (c), and after incubation in pD 5.0 buffer for 3 d (d).

physiological environment and the extracellular environment of the acidic tumor, we incubated HepG2 cells with free rhodamine B or host-1/rhodamine B inclusion complex for 1 h at pH 7.4, 6.4 or 5.5, respectively. We then washed the cells with PBS solution in order to clean the dyes that were not taken up by the cells for subsequent experimental measurements. We used high-throughput cell analyzers to observe cells and measure the uptake of Rhodamine B by HepG2 cells under different conditions. As shown in Fig. 9, at pH 7.4, free Rhodamine B cell uptake is more effective than host-1/Rhodamine B inclusion complex, because host-1 can encapsulate drugs and reduce their intracellular differentiation efficiency. In contrast, the uptake of fluorescent substances by the cells at pH 6.4 and 5.5 was significantly higher than pH 7.4. This is because host-1 rapidly cleaves and releases cargo in

Table 2
Cytotoxic activities of drugs and inclusion complex in vitro (IC_{50}, μM[a]).

	HCT116	HepG2	SY5Y	293T
POD	0.031	0.187	0.043	1.225
VP-16	1.255	16.88	2.45	16.34
host-1	> 100	> 100	> 100	> 100
POD/host-1 inclusion complex	8.617	3.519	7.53	> 100
VP-16/host-1 inclusion complex	5.931	19.05	13.24	> 100
Doxorubicin	0.26	6.35	5.45	1.81
Cisplatin	8.13	27.2	13.38	2.17

[a] The concentrations of free drugs and inclusion complexes mentioned in this table are as per mole of drugs.

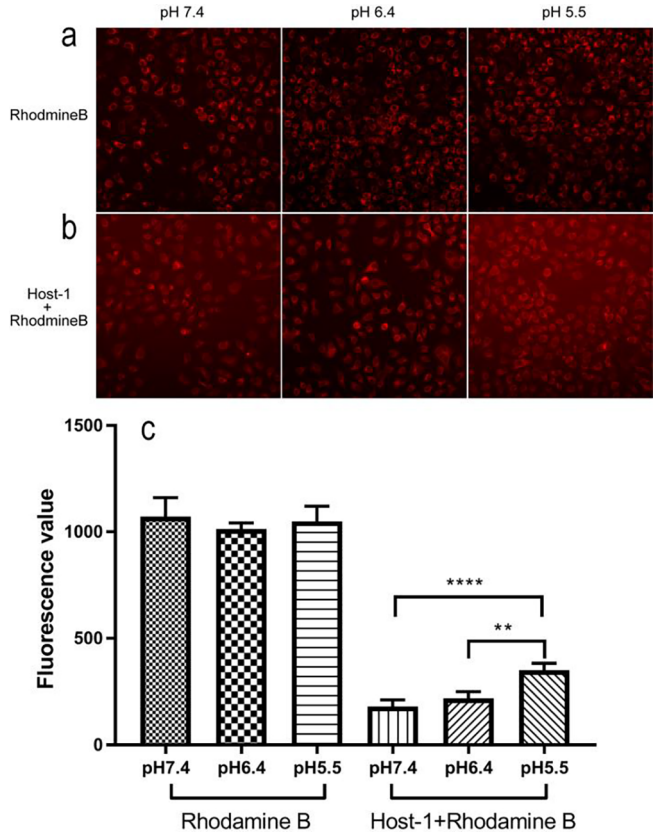

Fig. 9. pH-dependent cellular delivery of rhodamine B by host-1. Fluorescence imaging for cellular uptake of rhodamine B at different pH. (a) free rhodamine B, (b) host-1/rhodamine B inclusion complex. The concentrations of free rhodamine B (20 μg/ml) and inclusion complexes mentioned are as per mole of rhodamine B, (c) Intracellular fluorescence value. Data are expressed as the mean ± S.D. (n = 6, $^{**}P < 0.005$, $^{****}P < 0.0001$).

the cavity under acidic conditions, and Rhodamine B is effectively internalized by HepG2 cells. At the same time, we could observe that free rhodamine B was incubated at different pH conditions, and the uptake efficiency of rhodamine B in HepG2 cells was basically the same. Then we quantified Rhodamine B uptake by HepG2 cells. As shown in Fig. 9c, at pH 6.4 and 5.5, rhodamine B was stably controlled release in the inclusion complex. In contrast, when the clathrate was incubated at pH 7.4, Rhodamine B was stably encapsulated to have inefficient cellular internalization. Thus, the acid-controlled release complex strategy results in controlled release of the encapsulated drug at an accommodating rate at acidic pH, which enables targeted delivery of HepG2 cells incubated under mild acidic conditions.

4. Conclusion

In this work, acid-controlled release complexes of POD and VP-16 with pH-labile acyclic cucurbit[*n*]urils were successfully designed and prepared, and their acid-controlled characterizations and inclusion complexation behaviors have been confirmed. MTT assay indicates that antitumor activity of complexes was less toxic than that of raw dug, and cellular experiments indicate that complexes can release model drug (rhodamine B dye) in physiological pH environment of cancer cells. These studies provide strategies for targeting and responsive systems for better anticancer activity and low cytotoxic anticancer drugs for clinical applications.

Acknowledgments

This work was supported by Yunnan Applied Basic Research Projects (No. 2018FA047 and 2018FB018), and the National Natural Science Foundation of China (NNSFC), (No. 21362016, 21642001, 21361014 and 21302074), which are gratefully acknowledged.

Conflict of interest

The authors declare no conflict of interest.

Appendix A. Supplementary data

Supplementary data to this article can be found online at https://doi.org/10.1016/j.bmc.2018.12.035.

References

1. Zhang B, Isaacs L. Acyclic cucurbit[n]uril-type molecular containers: influence of aromatic walls on their function as solubilizing excipients for insoluble drugs. *J Med Chem.* 2014;57:9554–9563.
2. Zhou J, Yu G, Huang F. Supramolecular chemotherapy based on host-guest molecular recognition: a novel strategy in the battle against cancer with a bright future. *Chem Soc Rev.* 2017;46:7021–7053.
3. Mao D, Liang Y, Liu Y, et al. Acid-labile acyclic cucurbit[n]uril molecular containers for controlled release. *Angew Chem Int Ed.* 2017;129:12788–12792.
4. Chen J, Liu Y, Mao D, et al. Acyclic cucurbit [n] uril conjugated dextran for drug encapsulation and bioimaging [J]. *Chem Commun.* 2017;53:8739–8742.
5. Jiang S, Lan S, Mao D, et al. Pro-guest and acyclic cucurbit [n] uril conjugated polymers for the controlled release of anti-tumor drugs. *Chem Commun.* 2018;54:9486–9489.
6. Jackson DE, Dewick PM. Tumour-inhibitory aryltetralin lignans from Podophyllum pleianthum. *Phytochemistry.* 1985;24:2407–2409.
7. Zhang X, Rakesh KP, Shantharam CS, et al. Podophyllotoxin derivatives as an excellent anticancer aspirant for future chemotherapy: a key current imminent needs. *Bioorg Med Chem.* 2018;26:340–355.
8. You Y. Podophyllotoxin derivatives: current synthetic approaches for new anticancer agents. *Curr Pharm Des.* 2005;11:1695–1717.
9. Canel C, Moraes RM, Dayan FE, et al. *Podophyllotoxin Phytochem.* 2000;54:115–120.
10. Charlton JL. Antiviral activity of lignans. *J Nat Prod.* 1998;61:1447–1451.
11. Sudo K, Konno K, Shigeta S, et al. Inhibitory effects of podophyllotoxin derivatives on herpes simplex virus replication. *Antiviral Chem Chemother.* 1998;9:263–267.
12. Gordaliza M, Garcıa PA, Del Corral JMM, et al. Podophyllotoxin: distribution, sources, applications and new cytotoxic derivatives. *Toxicon.* 2004;44:441–459.
13. Samaratunga, Weedon David, Musgrave Nicholas, McCallum Naomi H. Atypical presentation of herpes simplex (chronic hypertrophic herpes) in a patient with HIV infection. *Pathology.* 2001;33:532–535.
14. Von Krogh G, Longstaff E. Podophyllin office therapy against condyloma should be abandoned. *Sex Transm Infect.* 2001;77:409–412.
15. Lacey CJN, Goodall RL, Tennvall GR, et al. Randomised controlled trial and economic evaluation of podophyllotoxin solution, podophyllotoxin cream, and podophyllin in the treatment of genital warts. *Sex Transm Infect.* 2003;79:270–275.
16. Donovan B. Sexually transmissible infections other than HIV. *Lancet.* 2004;363:545–556.
17. Yan J, Chen SL, Wang HN, et al. Meta-analysis of 5% imiquimod and 0.5% podophyllotoxin in the treatment of condylomata acuminata. *Dermatology.* 2006;213:218–223.
18. Gao Y, Han K, Wang Q, et al. Development of podophyllotoxinloaded nanostructured lipid carriers for the treatment of condyloma acuminatum. *Mol Med Rep.* 2018;17:6506–6514.
19. Gao Y, Han K, Wang Q, et al. Podophyllotoxin directly binds a hinge domain in E2 of HPV and inhibits an E2/E7 interaction in vitro. *Bioorg Med Chem.* 2008;16:5815–5825.
20. Kamal A, Ali Hussaini SM, Rahim A, et al. Podophyllotoxin derivatives: a patent review (2012–2014). *Expert Opin Ther Pat.* 2015;25:1025–1034.
21. Gordaliza M, Castro MA, Miguel del Corral JM, et al. Antitumor properties of podophyllotoxin and related compounds. *Curr Pharm Des.* 2000;6:1811–1839.
22. Antúnez-Mojica M, Rodriguez-Salarichs J, Redondo-Horcajo M, et al. Structural and biochemical characterization of the interaction of tubulin with potent natural analogues of podophyllotoxin. *J Nat Prod.* 2016;79:2113–2121.
23. Roy A, Ernsting MJ, Undzys E, et al. A highly tumor-targeted nanoparticle of podophyllotoxin penetrated tumor core and regressed multidrug resistant tumors. *Biomaterials.* 2015;52:335–346.
24. Zhang QY, Zhao W, Tang YJ. Discover the leading compound of 4β-S-(5-fluorobenzoxazole)-4-deoxy-4′-demethylepipodophyllotoxin with millimolar-potency toxicity by modifying the molecule structure of podophyllotoxin. *Eur J Med Chem.* 2018;158:951–964.
25. Wang Y, Sun H, Xiao Z, et al. DNA damage and apoptosis induced by a potent orally

podophyllotoxin derivative in breast cancer. *Cell Commun Signal.* 2018;16:52–64.
26. Sathish M, Kavitha B, Nayak VL, et al. Synthesis of podophyllotoxin linked β-carboline congeners as potential anticancer agents and DNA topoisomerase II inhibitors. *Eur J Med Chem.* 2018;144:557–571.
27. Liu YQ, Tian J, Qian K, et al. Recent progress on C-4-modified podophyllotoxin analogs as potent antitumor agents. *Med Res Rev.* 2015;35:1–62.
28. Cheng WH, Cao B, Shang H, et al. Synthesis and evaluation of novel podophyllotoxin derivatives as potential antitumor agents. *Eur J Med. Chem.* 2014;85:498–507.
29. Aisner J, Lee EJ. Etoposide etoposide. current and future status. *Cancer.* 2016;22:692–696.
30. Reck M, Luft A, Szczesna A, et al. Phase III randomized trial of ipilimumab plus etoposide and platinum versus placebo plus etoposide and platinum in extensive-stage small-cell lung cancer. *J Clin Oncol.* 2016;34:3740–3748.
31. Zeng J, Yang L, Huang F, et al. The metronomic therapy with prednisone, etoposide, and cyclophosphamide reduces the serum levels of VEGF and circulating endothelial cells and improves response rates and progression-free survival in patients with relapsed or refractory non-Hodgkin's lymphoma. *Cancer Chemother Pharm.* 2016;78:801–808.
32. Muggia FM, Russell CA. Russell, New chemotherapies for ovarian cancer. systemic and intraperitoneal podophyllotoxins. *Cancer.* 1991;67:225–230.
33. Fleming RA, Miller AA, Stewart CF. Etoposide: an update. *Clin Pharm.* 1989;8:274–293.
34. Guo Y, Zhang Y, Li J, et al. Inclusion complex of podophyllotoxin with γ-cyclodextrin: preparation, characterization, anticancer activity water-solubility and toxicity. *Chin J Chem.* 2016;34:425–431.
35. Zhang B, Zavalij PY, Isaacs L. Acyclic CB[n]-type molecular containers: effect of solubilizing group on their function as solubilizing excipients. *Org Biomol Chem.* 2014;12:2413–2422.
36. Huang CY. Determination of binding stoichiometry by the continuous variation method: the job plot. *Methods Enzymol.* 1982;87:509–525.
37. Kirby AJ, Lancaster PW. Structure and efficiency in intramolecular and enzymic catalysis. Catalysis of amide hydrolysis by the carboxy-group of substituted maleamic acids. *J Chem Soc Perkin Trans 2.* 1972;9:1206–1214.